

IDENTIFICATION OF THE ELECTRONIC-VIBRATIONAL-ROTATIONAL SPECTRUM OF THE HO₂ RADICAL IN THE REGION 1.22–1.27 μm

V.P. Bulatov, F.N. Dzegilenko, V.A. Lozovskii, Yu.V. Matyagin, O.M. Sarkisov,
and E.A. Sviridenkov

*Institute of Chemical Physics,
Academy of Sciences of the USSR, Moscow
Received March 15, 1989*

The high-resolution electronic-vibrational-rotational spectrum of the ${}^2A' \leftarrow {}^2A''$ electronic transition of the HO₂ radical in the region 1.22–1.27 μm was studied. The spectrum was obtained by the method of intracavity laser spectroscopy. The spectrum was calculated using Polo's formulas for slightly asymmetric prolate tops. Analysis of the spectra yielded accurate values for the rotational constants of the $\tilde{A}^2 A'(001)$ and $\tilde{A}^2 A'(020)$ states and the vibrational frequencies ν_0 and ν_3 of the $\tilde{A}^2 A'$ state. It was established that the forbidden $\Delta K = 0$ transitions occur. A possible mechanism (Coriolis interaction of the close-lying ${}^2A'(001)$ and ${}^2A'(010)$ levels) explaining their appearance is proposed. It is shown based on calculations that vibrationally excited HO₂ radicals are formed in the ${}^2A''(010)$ state via the reaction $\text{CH}_3\text{O} + \text{O}_2 \rightarrow \text{CH}_2\text{O} + \text{HO}_2$.

1. INTRODUCTION

The free radical HO₂ has been under intense study for the last few years. The necessity for studying this radical is explained by the fact that it is a very important intermediate product in the combustion and transformation of different impurities in the atmosphere. The HO₂ radical was first detected spectroscopically in Ref. 1, where the IR-spectrum in an argon matrix was obtained. In Refs. 2–4 it was identified in the gas phase based on the UV-absorption. The UV-absorption spectrum in the region 1800–2700 Å is continuous and has a maximum at about 2100 Å. Walsh predicted the existence of a low-lying electronic state.⁵ In 1974 Becker and Fink⁶ obtained the near-IR emission spectrum in the interval 1.2–2.1 μm in the reaction system O/O₂(¹Δ_g)/C₂H₄. The strongest band in the 1.43 μm region was ascribed to the transition ${}^2A'(000) \rightarrow {}^2A''(000)$ of the HO₂ radical. In Ref. 7 some of the same bands were obtained by the method of absorption spectroscopy using mercury-photosensitized decomposition of hydrogen in the presence of oxygen to obtain the HO₂ radical. Because of their low resolution both studies gave little spectroscopic information about the first excited state of the HO₂ radical and confirmed only Walsh's data.⁵

An intermediate-resolution emission spectrum of the bands ${}^2A'(001) \rightarrow {}^2A''(000)$ of the radicals HO₂ and DO₂ were obtained in Ref. 8. Becker and Fink⁸ were able to determine the energies of the vibrational levels for both electronic states ${}^2A''$ and ${}^2A'$ right up to $\nu_3 = 3$ and $\nu' = 6$, respectively.

A high-resolution emission spectrum of the band ${}^2A' \rightarrow {}^2A''$ in the region 1.43 μm was first obtained in Ref. 9, but the signal/noise ratio was too low. A much

better emission spectrum in the region 1.43–1.51 μm was obtained in Ref. 10. A high-resolution spectrum of the HO₂ radical in the region 1.22–1.27 μm has not been obtained up to now.

In this paper we examine the high-resolution electron-vibrational-rotational absorption spectrum of the HO₂ radical in the region 1.22–1.27 μm. The spectrum was obtained by the method of intracavity laser spectroscopy (ICLS) using a spectrometer with an F₂⁻ color center laser.¹¹

The detection of peroxide radicals by the ICLS method, in which high sensitivity is combined with high spectral and temporal resolution, gives a new method of diagnostics and study of processes involving peroxide radicals that has a number of advantages over UV detection.

2. EXPERIMENTAL CONDITIONS FOR OBTAINING THE SPECTRUM OF THE HO₂ RADICAL

The method of IR ICLS employed in this work to record the spectrum in the 1.25 μm region is described in Ref. 11. The absorption spectra of HO₂ radicals (the transition ${}^2A' \leftarrow {}^2A''$) in the region 1.22–1.27 μm was recorded using a laser with an active element based on F₂⁻ – color centers in an LiF crystal. The arrangement of the apparatus is shown in Fig. 1.

The laser cavity is formed by two spherical mirrors (2.5). The active element was optically pumped in an almost longitudinal scheme by radiation from a neodymium laser which operated in the free-lasing mode. The lasing parameters of the pump laser were selected so as to obtain spike-free lasing of the crystal in the entire spectral tuning range. A prism (4), consisting

of heavy flint, was inserted into the cavity in order to be able to tune the lasing spectrum continuously. The tuning was performed by rotating the mirror (5). Tuning was performed in the range 1.1–1.28 μm with a laser spectrum width of 3–15 nm. The lasing time ranged from 80 to 200 μs . A reaction cell (3), consisting of a quartz cylinder 1.6 cm in diameter and 15 cm long, was placed inside the cavity. Photolysis of the reaction mixture was performed by radiation from two IFP-200 xenon flashlamps with up to 400 J of electrical energy per pulse. The probe pulse of the F_2^- color center laser was injected following photolysis after a regulatable delay time. Radiation was extracted from the laser cavity by means of reflection from one of the working surfaces of the crystal, which was bevel led at an angle of 5° to the axis of the resonator.

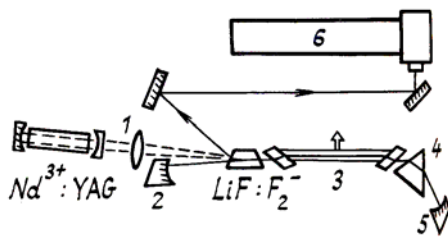


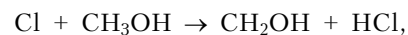
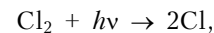
FIG. 1. Arrangement of the experimental apparatus: 1) focusing system; 2, 5) cavity mirrors of the color-center laser; 3) reaction cell; 4) prism; 6) spectrograph.

The lasing spectrum of the color-center laser was recorded photographically on 1–3 film with the help of a laboratory diffraction spectrograph (6), assembled based on a UF-90 autocollimation camera.

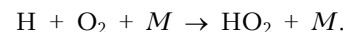
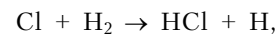
The effective resolution was equal to 0.02 nm ($\approx 0.13 \text{ cm}^{-1}$) and the inverse dispersion was equal to 4.1–4.8 nm/cm. The absorption spectrum was referenced to the wavelengths in the tuning range of the laser based on the absorption spectrum of the atmosphere¹² and the emission lines of electrodeless neon lamps with conversion of the wavelengths into the required order. The spectra obtained were analyzed on an IFO-451 microphotometer.

Photolysis of mixtures of chlorine, oxygen, and methyl alcohol (or hydrogen) with the following compositions were employed as the source of HO_2 radicals: Cl_2 (0.2–0.5 torr), CH_3OH (0.1–2.5 torr) and O_2 (9–15 torr) or Cl_2 (3–4 torr), H_2 (50–100 torr) and O_2 (400 torr).

Such methods for obtaining HO_2 radicals are well known and widely employed. The HO_2 radicals are formed as a result of the following reactions:



or



The spectrum presented in Fig. 2 was obtained under the following conditions:

Cl (1.0 torr), CH_3OH (0.4 torr), O_2 (10 torr).

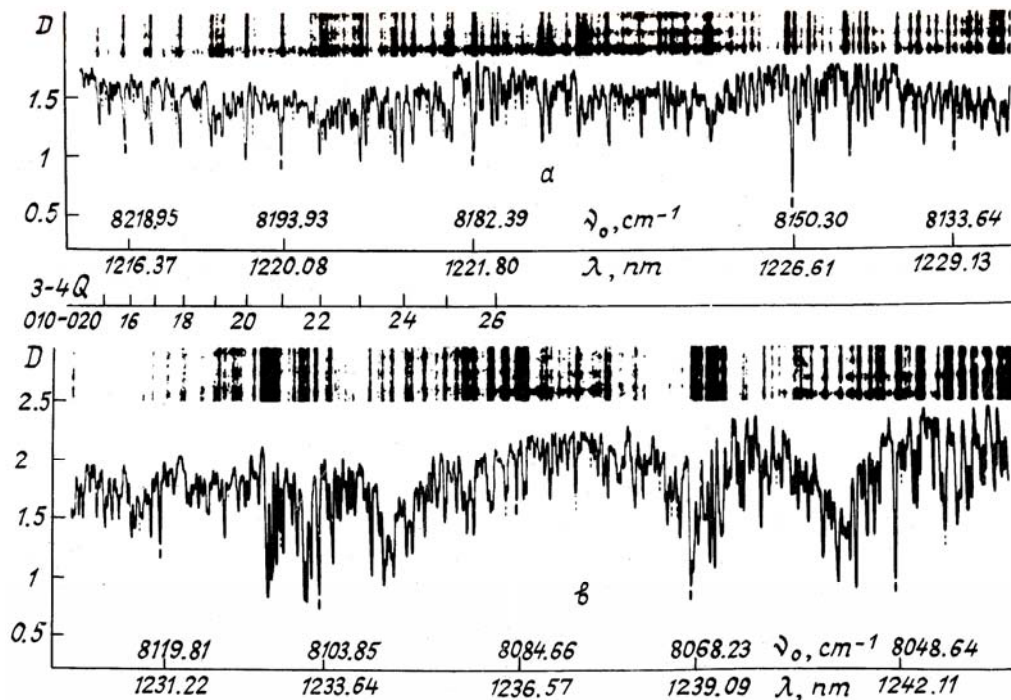


FIG. 2. The spectrum of the HO_2 radical in the region 1.22–1.27 μm

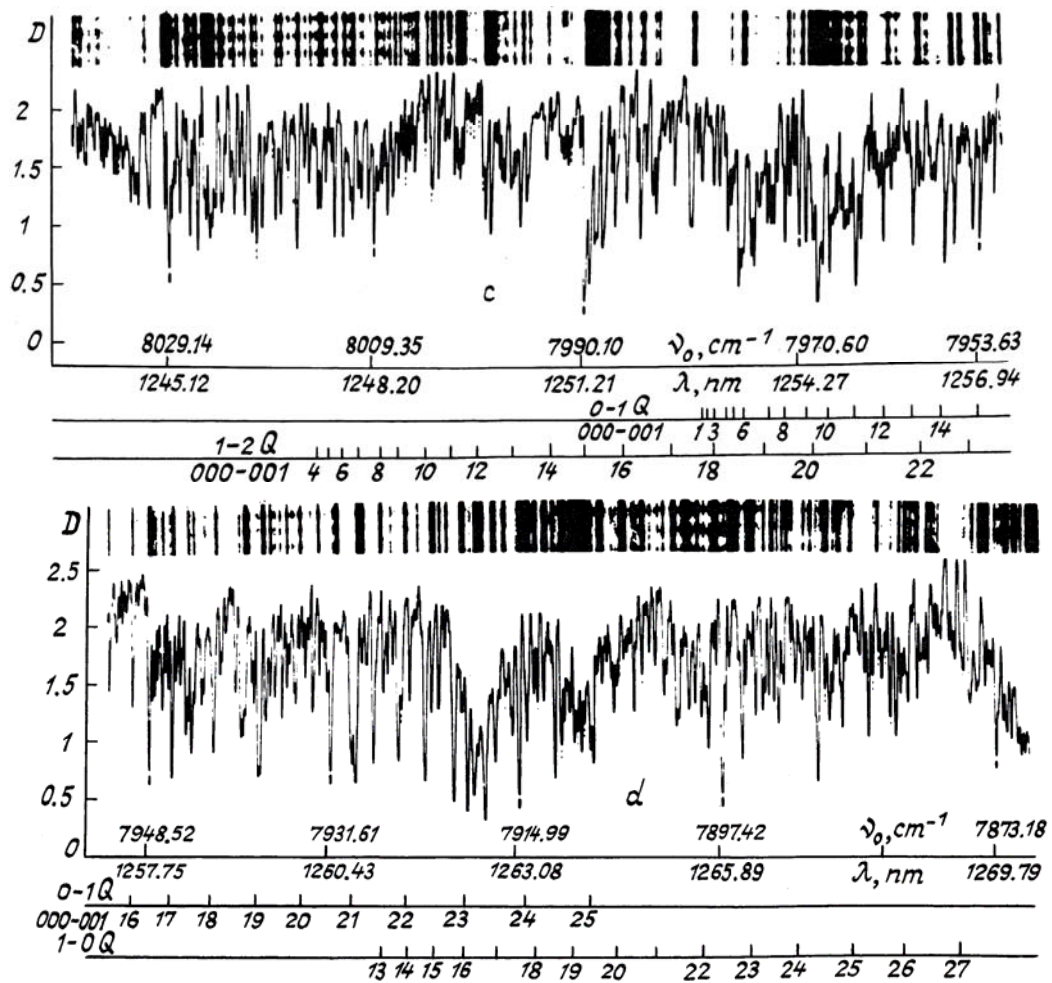


Fig. 2. Continuation

In observations of the spectrum with different time delays after the photolyzing pulse it was found that the spectrum vanishes after about $4 \cdot 10^3 \mu\text{s}$, i.e., the lifetime of the observed intermediate state is short. In addition, adding nitrogen oxide to the reaction mixture sharply reduced the lifetime of this compound. The spectrum was not observed when any component of the mixture was not present in the cell. Further, the observed lines were found in the region $1.22\text{--}1.27 \mu\text{m}$, which is also the region of the maximum of the absorption band $\text{HO}_2 \ ^2A'(001) \rightarrow \ ^2A''(000)$.⁸

We observed the identical spectrum in the system $\text{CO}_2 - \text{H}_2 - \text{O}_2$,¹¹ and HO_2 must be regarded as the only radical common to both systems.

To confirm finally the fact that the observed spectrum belongs to the HO_2 radical Bulatov et al.¹¹ performed experiments with deuterated methanol. Since the HO_2 radicals are formed from the oxygen present in the mixture and the hydrogen atoms from the hydroxyl group of methanol, when the hydrogen atom is replaced by a deuterium atom one would expect the appearance of the radical DO_2 . Indeed, with the use of the alcohols CH_3OD and CD_3OD a spectrum with a different arrangement of the lines and ratio of intensities was recorded: the DO_2 spectrum

($\ ^2A' \leftarrow \ ^2A''$). In Ref. 11 when CD_3OH was used the spectrum of the HO_2 radical was observed once again. Thus, using kinetic methods, Bulatov et al.¹¹ showed that the observed spectrum belonged to the HO_2 radical.

3. ANALYSIS OF THE SPECTRUM OF THE HO_2 RADICAL

We shall study the rotational structure of the electronic transition $A^2A' \leftarrow \tilde{X}^2A''$ of the HO_2 radical. Taking into account the centrifugal deformation the rotational term $F(N, K)$ of nearly a prolate symmetric top molecules is described by the formula¹³:

$$F(N, K) = \frac{B+C}{2}N(N+1) + \left[A + \frac{B+C}{2} \right] \cdot \left[1 - \frac{3}{8}b^2 \right] K^2 + \\ + \Delta B_{\text{eff}}^K \cdot N(N+1) + \Delta D_{\text{eff}}^K \cdot N^2(N+1)^2 - D_K K^4 - D_{NK} N(N+1)K^2 - \\ - D_N \cdot N^2(N+1)^2, \quad (1)$$

where A is a rotational constant, corresponding to the rotation around the axis of the top; the axis of the top practically coincides with the 0-0 bond in the HO_2

molecule; B is a rotational constant corresponding to the rotation around an axis perpendicular to the axis of the top, but lying in the plane of HO_2 ; C is a rotational constant corresponding to the rotation around an axis perpendicular to the plane of the radical (the z -axis);

$b = \frac{C-B}{2A-B-C}$ is the asymmetry parameter; D_K ,

D_{NK} , and D_N are the centrifugal stretching constants; ΔB_{eff}^K and ΔD_{eff}^K are asymmetry constants which are functions of b and K and assume the following approximate values:

$$\Delta B_{\text{eff}}^K = \left[A - \frac{B+C}{2} \right] \frac{1}{4} b^2, \text{ for } K = 0 \text{ and } K \geq 3;$$

$$\left[A - \frac{B+C}{2} \right] \left[\pm \frac{1}{2} b + \frac{1}{4} b^2 \right] \text{ for } K = 1;$$

$$\left[A - \frac{B+C}{2} \right] \frac{1}{8} (2 \pm 1) b^2 \text{ for } K = 2;$$

$$\Delta D_{\text{eff}}^K = - \frac{1}{8} b^2 \left[A - \frac{B+C}{2} \right] \text{ for } K = 0;$$

$$\left[A - \frac{B+C}{2} \right] \left[- \frac{1}{32} b^2 \right] \text{ for } K = 1;$$

$$\left[A - \frac{B+C}{2} \right] \frac{1}{48} (2 \pm 3) b^2 \text{ for } K = 2;$$

$$0 \text{ for } K \geq 3. \quad (2)$$

The \pm sign in these formulas corresponds to K doubling. This doubling is maximal in levels with $K = 0$. It increases as N increases and decreases as K increases. For molecules with such weak asymmetry as the HO_2 molecule., all rotational levels with $K \geq 3$ can be regarded as unsplit.

The electronic transition ${}^2A' \leftarrow {}^2A''$ in the HO_2 molecule, studied in this work, is a transition of the C-type with the nonzero transition moment oriented perpendicular to the plane of the molecule. The selection rules for transitions of this type have the form

$$\Delta K = \pm 1 \text{ and } + + \leftrightarrow + -, - + \leftrightarrow - -$$

Using Polo's formulas¹³ and the selection rules for electronic-vibrational-rotational transitions we analyzed some of the subbands observed in the spectrum of HO_2 , independently of one another. By reducing the observed wave numbers of the lines to the expression

$$\nu = \nu^0 + XN(N+1) + YN^2(N+1)^2$$

we were able to obtain the effective values of ν^0 , X , and Y , from which we then obtained the true values of the rotational constants. The reduction of the experimental values of the wave numbers of the lines of all branches in the ${}^2A' \leftarrow {}^2A''$ electronic band to a quadratic form was performed by the method of least squares (MLS). The second possible method for determining the rotational constants — the method of combination differences —

was not employed in this work owing to the difficulty of identifying the weak lines of the P and R branches.

3.1. ANALYSIS OF THE ${}^2A'(0.001) \leftarrow {}^2A''(000)$ ELECTRONIC BAND OF THE RADICAL HO_2

The most noticeable feature of the spectrum is the very strong sequence of lines starting at $\approx 7972 \text{ cm}^{-1}$, which was ascribed to the $K'' = 0 \rightarrow K' = 1$ Q-branch. The $K'' = 1 \rightarrow K' = 0$ Q-branch, the intensity of whose lines reaches a maximum in the region 7919.5 cm^{-1} (Fig. 2), is less noticeable in the spectrum.

TABLE I. The molecular constants of HO_2 ${}^2A'(v_1v_2v_3) \leftarrow {}^2A''(v_1v_2v_3) \text{ cm}^{-1}$

Parameter	000-000	010-010	001-001
A''	20.357 ^c	20943 ^b	20.309 ^e
B''	1.1179 ^c	1.1156 ^b	1.1072 ^a
C''	1.1156 ^c	1.0493 ^b	1.0350 ^a
$D_{N''}$	$3.93 \cdot 10^{-6d}$	$3.94 \cdot 10^{-6b}$	—
$D_{NK''}$	$1.156 \cdot 10^{-4d}$	$1.114 \cdot 10^{-4b}$	—
$D_{K''}$	$4.1/10^{-3d}$	$5.156 \cdot 10^{-3b}$	—
A'	1.0218 ^a	22.957 ^a	19.740 ^a
B'	1.0218 ^a	1.0253 ^a	1.0055 ^a
C'	0.9690 ^a	0.9727 ^a	0.9526 ^a
$D_{N'}$	$5.20 \cdot 10^{-6a}$	—	—
$D_{NK'}$	$1.20 \cdot 10^{-4a}$	—	—
$D_{K'}$	$4.10 \cdot 10^{-3a}$	—	—
ν_0	7029.48 ^a	6924.22	6916.67
Frequency of vib. in ${}^2A''$	—	1390 ^a	1097.6 ^e
Frequency of vib. in ${}^2A'$	—	1285 ^a	984.8 ^a

Note. a) according to the data of Ref. 10; b) Ref. 16; c) Ref. 15; d) Ref. 14; and, e) Ref. 17.

Using the results of reduction of the lines of the strongest $K'' = 0 \rightarrow K' = 0$ Q-branch to the quadratic form $N(N+1)$ as well as more accurate values of the rotational constants for the ground state (Refs. 14 and 15, Table I), we obtained the following values for the rotational constants of the ${}^2A'(001)$ state:

$$A' = 19.74 \pm 0.074 \text{ cm}^{-1}; D_{N'} = 1.1044 \cdot 10^{-5} \text{ cm}^{-1};$$

$$B' = 1.019 \pm 0.000 \text{ cm}^{-1}; D_{NK'} = 1.2 \cdot 10^{-4} \text{ cm}^{-1};$$

$$C' = 0.9661 \pm 0.000 \text{ cm}^{-1}; D_{K'} = 4.1 \cdot 10^{-3} \text{ cm}^{-1};$$

$$\nu_0({}^2A'(001) \leftarrow {}^2A''(000)) = 7960.938 \pm 0.074 \text{ cm}^{-1};$$

$$\nu_3({}^2A'(001) \leftarrow {}^2A''(000)) = 931.46 \pm 0.074 \text{ cm}^{-1};$$

The values obtained for the rotational constants and the vibrational frequencies enabled us to calculate completely the structure of the ${}^2A'(001) \leftarrow {}^2A''(000)$ band. Comparing the computed values of the wave numbers with the experimental data we also described (aside from $K'' = 0 \rightarrow K' = 0$ and $K'' = 1 \rightarrow K' = 0$ Q) also some other weaker branches. We did not observe spin splitting in any of the branches described.

$\Delta K = 0$ transitions (parallel band). In Refs. 7 and 10 it was observed in an analysis of the ${}^2A'(000) \leftarrow {}^2A''(000)$ emission band that anomalous unidentified lines were present near the start of the band. In Ref. 10 all anomalous lines were ascribed to the R-branches of the forbidden $\Delta K = 0$ transitions. We also observed an analogous pattern in the analysis of the ${}^2A'(001) \leftarrow {}^2A''(000)$ perpendicular band. It should be noted that in analyzing the spectrum it is difficult to establish whether or not the anomalous lines ($\Delta K = 0$) observed in the spectrum belong to transitions of the type $++ \Leftrightarrow -+$, $+ - \Leftrightarrow - -$ or $++ \Leftrightarrow ++$, $- + \Leftrightarrow - +$ owing to the closeness of the values of the wave numbers of the corresponding lines. In analyzing the spectrum, however, we were able to observe a quite strong $K'' = 0 \rightarrow K' = 0$ Q-branch. Its appearance would be impossible, if the transitions obey the selection rules $++ \Leftrightarrow -+$. Based on this it was concluded that all anomalous lines belong to transitions of the type $++ \Leftrightarrow ++$ and $- + \Leftrightarrow - +$, which are forbidden in accordance with the selection rules presented above.

3.2 ANALYSIS OF THE ${}^2A'(020) \rightarrow {}^2A''(010)$ TRANSITION

In analyzing the ${}^2A'(001) \leftarrow {}^2A''(000)$ band we were not able to associate the quite strong and well-resolved system of lines in the high-frequency of the spectrum at 8240 cm^{-1} with any branches of the indicated band. The only transition which could have been realized in this I spectral region for the HO^{*} molecule is the hot l transition ${}^2A'(020) \leftarrow {}^2A''(010)$. Because of the fact that this transition has not been observed by anyone, there were also no data on the rotational constants of the upper ${}^2A'(020)$ state. Making the assumption that the rotational constants of the ${}^2A'(020)$ state do not differ much from the analogous values for the ${}^2A'(010)$ state, which were determined in Ref. 10, we calculated to a first approximation the rotational structure of the hot transition ${}^2A'(020) \leftarrow {}^2A''(010)$. Based on the calculations performed we established that the system of lines observed near 8240 cm^{-1} could be associated with the $K'' = 3 \rightarrow K' = 4$ Q-branch of the transition ${}^2A'(020) \leftarrow {}^2A''(010)$. Subsequent MLS analysis of this branch enabled us to calculate the effective values of the rotational constants v^0 , X, and Y, from which we obtained the following values of the molecular constants of the ${}^2A'(020)$ state:

$$A' = 22.957 \pm 0.052 \text{ cm}^{-1};$$

$$B' = 1.0284 \pm 0.000 \text{ cm}^{-1};$$

$$C' = 0.9755 \pm 0.000 \text{ cm}^{-1};$$

$$D' = 1.3729 \cdot 10 \text{ cm}^{-1};$$

$$v_0({}^2A'(020) \leftarrow {}^2A''(010)) = 8070.166 \pm 0.052 \text{ cm}^{-1};$$

$$v_2({}^2A'(020) \leftarrow {}^2A''(010)) = 1145.95 \pm 0.052 \text{ cm}^{-1};$$

We assumed, in so doing, that the values of D_{NK} and D_K not change in the transition ${}^2A'(020) \leftarrow {}^2A''(010)$. The values we obtained enabled us to evaluate the magnitude of the anharmonicity constant for the deformation vibration. It turned out to be equal to $X'_2 = -69.55 \text{ cm}^{-1}$.

Using the values obtained for the rotational constants of the ${}^2A'(020)$ state we repeated the calculation of the rotational structure of the band ${}^2A'(020) \leftarrow {}^2A''(010)$. Comparing the computed values and the experimental data of the wave numbers of the lines we able to describe (in addition to the $K'' = 3 \rightarrow K' = 4$ Q-branch) several other branches within the indicated transition (Table II).

For the ${}^2A'(020) \leftarrow {}^2A''(010)$ band we also observed the forbidden $\Delta K = 0$ transitions, whose intensity, however, was lower than for the corresponding transitions ${}^2A'(001) \leftarrow {}^2A''(000)$. We identified a total sum of about 850 lines. Some of them are given in Table II.

4. DISCUSSION

Analysis of the absorption bands in the $1.22\text{--}1.27 \text{ }\mu\text{m}$ region in the near-IR part of the spectrum enabled us to obtain a large amount of new spectroscopic information about the ${}^2A'$ electronic state of the HO₂ radical. Analysis revealed, however, two important problems: the presence of strong $\Delta K = 0$ lines in the ${}^2A' \leftarrow {}^2A''$ transition of the C-type and serious differences between our value of v_3 for the ${}^2A'$ state and the value presented in Ref. 10. We shall examine these questions in turn.

4.1 PRESENCE OF STRONG $\Delta K = 0$ LINES IN THE C-TYPE ${}^2A' \leftarrow {}^2A''$ TRANSITION

We also observed the presence of weak forbidden $\Delta K = 0$ bands in electronic transitions of the C-type $\Delta K = \pm 1$ for other triatomic molecules — HCO, HNF, HSiBr, and HSiCl. We attributed their appearance to the turning of the axes. The analysis performed in Ref. 10 showed, however, that the rotational constant A changes only from 20.358 to 19.74 cm^{-1} in the transition $\tilde{A}^2A' \leftarrow \tilde{X}^2A$ of the radical HO₂, and therefore the molecular geometry should not change significantly in this transition. This is confirmed by the small change in the HOO valence angle from 104° in the ${}^2A''$ electronic state to 192.7° in the ${}^2A'$ electronic state.¹⁰ As a result of this, the axis-turning mechanism cannot be the main reason for the appearance of the $\Delta K = 0$ lines the spectrum of HO₂.

Table II. The experimental and computed positions of the lines of the transition ${}^2A' \leftarrow {}^2A''$

N	Experimental positions of the lines, cm^{-1}	Difference between experiment and calculation	N	Experimental positions of the lines, cm^{-1}	Difference between experiment and calculation
1	2	3	1	2	3
${}^2A'(001) \leftarrow A''(000)$ transition					
$K'' = 0 \rightarrow K' = 1$ Q-branch					
1	7979.509	0.043	15	7953.675	0.037
2	7979.009	-0.024	16	7950.184	0.038
3	7978.410	0.024	17	7946.394	-0.037
4	7977.414	-0.107	18	7942.522	0.028
5	7976.561	0.121	19	7938.304	-0.026
6	7975.105	-0.037	20	7933.964	0.023
7	7974.503	-0.124	21	7929.492	0.167
8	7971.911	0.016	22	7924.564	0.083
9	7969.971	0.026	23	7919.509	0.101
10	7967.804	0.028	24	7914.289	0.185
11	7965.390	0.001	25	7908.571	0.003
12	7962.819	0.037	27	7896.813	0.015
13	7959.991	0.036	28	7890.656	0.096
14	7956.962	0.055			
$K'' = 1$ (low component) $\rightarrow K' = 1$ (upper component)					
R-branch					
2	7966.128	0.075	19	7974.212	0.046
5	7970.578	0.093	20	7973.167	-0.088
7	7972.662	-0.107	21	7972.146	-0.027
8	7973.753	0.063	22	7971.037	0.121
10	7975.105	-0.002	23	7969.477	0.000
11	7975.695	0.068	24	7967.804	-0.051
12	7975.903	-0.079	25	7966.128	0.082
13	7976.092	-0.097	26	7964.143	0.100
15	7976.092	-0.056	27	7961.799	-0.044
16	7975.903	0.008	28	7959.462	0.020
18	7974.949	0.042			
${}^2A'(020) \leftarrow {}^2A''(010)$ transition					
$K'' = 3 \rightarrow K' = 4$ Q-branch					
6	8238.421	0.051	18	8212.827	-0.028
7	8237.260	0.043	19	8209.469	-0.029
9	8234.480	0.074	20	8205.982	0.048
10	8232.837	0.096	21	8202.131	-0.025
12	8228.843	-0.037	22	8198.139	-0.024
13	8226.626	-0.055	23	8193.934	-0.013
14	8224.291	-0.006	24	8189.624	0.009
15	8221.720	-0.007	26	8179.950	0.036
16	8218.952	-0.013	27	8174.665	-0.088
17	8216.022	0.012			
$K'' = 1$ (upper component) $\rightarrow K' = 1$ (low component)					
R-branch					
4	8079.842	-0.087	18	8070.571	-0.069
5	8080.749	-0.045	19	8068.224	0.113
6	8081.543	0.110	20	8065.331	-0.087
8	8081.983	-0.041	21	8062.269	0.030
9	8081.983	0.009	23	8055.173	-0.079
12	8080.341	-0.066	24	8051.308	-0.020
16	8074.868	-0.043	26	8042.544	-0.046
17	8072.930	0.024	27	8037.708	-0.056

Other factors, such as taking into account the off-diagonal elements of the spin-rotational interaction tensor in the ${}^2A'$ electronic state of HO_2 (Ref. 14) and the Renner-Teller interaction between the vibrational level of the ${}^2A'$ and ${}^2A''$ electronic states,¹⁰ also cannot explain a number of phenomena that we observed in the analysis of the spectrum of the HO_2 radical (for example, the fact that the $\Delta K = 0$ transitions for ${}^2A'(001) \leftarrow {}^2A''(000)$ are not weaker than the analogous transitions for ${}^2A'(000) \leftarrow {}^2A''(000)$). For this reason we proposed that the interaction of the rotation with the electronic-vibrational motion, i.e., the Coriolis interaction of the ${}^2A'(001)$ and ${}^2A'(010)$ levels, the splitting between which is $\approx 250 \text{ cm}^{-1}$ is mainly responsible for the appearance of the strong $\Delta K = 0$ lines. This proposition is in agreement with Jahn's rule, according to which two vibrations of a rotating molecule will interact as a result of the appearance of Coriolis forces only in the case when the product of their electronic-vibrational symmetry types contains the rotational symmetry type.¹⁸

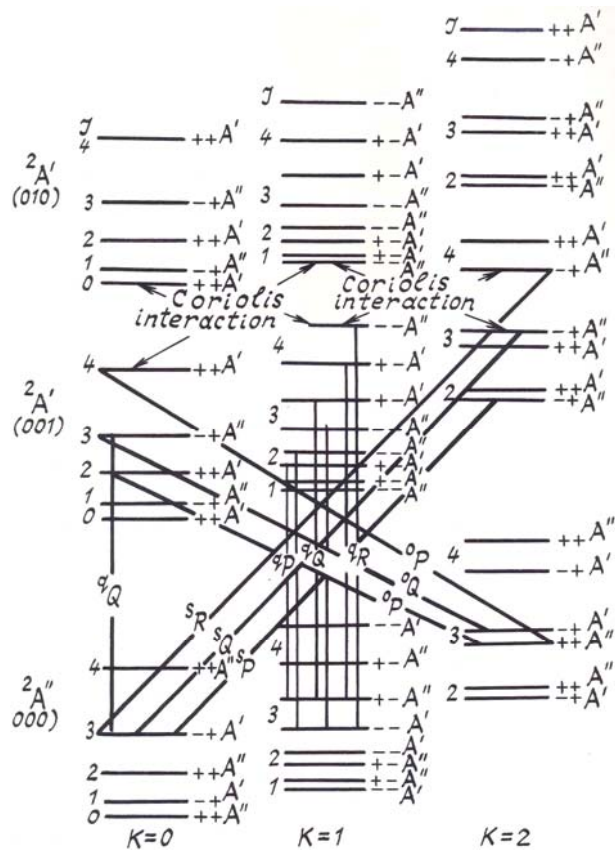


FIG. 3. The transitions between the rotation levels owing to the Coriolis interaction of the ${}^2A'(010)$ and ${}^2A'(001)$ electronic-vibrational states. The arrows connect the electronic-vibrational states whose rotational levels interact with one another. The interacting rotational levels have the same values of J .

Consider the electronic-vibrational transition ${}^2A'(001) \leftarrow {}^2A''(000)$. Since the ${}^2A'(010)$ state, which

can interact with the ${}^2A'(001)$ state, lies adjacent to the ${}^2A'(001)$ state it turns out that a transition from the upper rotational levels of the ${}^2A'(001)$ state to the levels of the ${}^2A'(010)$ state is possible. Since the mixing is due to rotation around the Z-axis levels with values of K differing by ± 1 can perturb one another.¹³ Figure 3 shows a diagram of the energy levels for this case.

The Coriolis interaction can occur only between states with identical values of J (or N) having the same electronic-vibrational-rotational types of symmetry (the latter are indicated in Fig. 3 next to the corresponding symmetry properties of the rotational wave functions).

As one can see from Fig. 3 the electronic-vibrational levels of the ${}^2A'(001)$ state with $K = 0$ mix with the levels of the ${}^2A'(010)$ state with $K = 1$; the levels of the ${}^2A'(001)$ state with $K = 0$ and 2, etc. For this reason transitions with $\Delta K = 0$ and ± 2 are possible, i.e., q , s , and o branches form in the subbands. The transitions obey the selection rules $++ \leftrightarrow ++$, $-+ \leftrightarrow -+$, $-- \leftrightarrow --$ and $+- \leftrightarrow +-.$ These transitions are forbidden by the selection rules presented above for the types of symmetry of an asymmetric top. These selection rules are, however, not strict; but, strict selection rules however, satisfied for the electronic-vibrational-rotational types of symmetry in spite of the breakdown of the selection rules for the rotational types of symmetry (according to the rules for the electronic-vibrational-rotational types of symmetry for molecules of the point symmetry group C_s the transition $A'' \rightarrow A'$ is an allowed electronic-vibrational-rotational transition¹³).

Thus the proposed mechanism apparently explains not only the appearance of transitions with $\Delta K = 0$ in the spectrum, but also the fact that the observed transitions obey "anomalous" selection rules $++ \leftrightarrow ++$ and $-+ \leftrightarrow -+.$

4.2. DIFFERENCES IN ν_3 FOR THE HO_2 RADICAL (${}^2A'$)

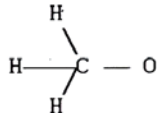
Our value $\nu_3 = 931.46 \text{ cm}^{-1}$ agrees with the results of the investigation of the absorption spectrum of HO_2 ,⁷ but disagrees seriously with the value $\nu_3 = 985 \text{ cm}^{-1}$ obtained in Ref. 10 in a study of the high-resolution emission spectrum. This value of ν_3 (Ref. 10) was obtained, however, in an analysis of the hot transition ${}^2A''(001) \rightarrow {}^2A''(001)$ i.e., it was evaluated only indirectly. Holstein et al.,¹⁹ for example, believe that at least some of the lines ascribed in Ref. 10 to the $\nu_3' = 1 \rightarrow \nu_3' = 1$ transitions from the lowest K' levels actually belong to the stronger $\nu_3' = 0 \rightarrow \nu_3' = 0$ transitions from high K' levels, so that in Ref. 10 ν_3 was not evaluated correctly.

4.3. UNASSIGNED LINES IN THE SPECTRUM

In analyzing the spectrum we observed a strong sequence of lines in the region $7917\text{--}7927 \text{ cm}^{-1}$ that could not be described by any of the branches of the

${}^2A'(020) \leftarrow {}^2A''(010)$ and ${}^2A'(001) \leftarrow {}^2A''(000)$ transitions. We conjecture that this sequence of lines can correspond to the $K = 0$ $K' = 1$ Q-branch of the hot transition ${}^2A'(002) \leftarrow {}^2A''(001)$.

We were also not able to describe the high-frequency edge in the region 8252.4 cm^{-1} . One radical in addition to HO_2 which, in our opinion, could give this edge is the radical CH_3O



5. CONCLUSIONS

Thus in this paper we studied the high-resolution absorption spectrum of the radical HO_2 in the region $1.22\text{--}1.27 \mu\text{m}$. We calculated the rotational structure of the bands $\tilde{A} {}^2A'(001) \leftarrow \tilde{X} {}^2A''(000)$ and $\tilde{A} {}^2A'(020) \leftarrow \tilde{X} {}^2A''(010)$ in the approximation of a weakly asymmetric prolate top and we obtained new spectroscopic data: the rotational constants of the ${}^2A'(001)$ and ${}^2A'(020)$ states and the vibrational frequencies ν_2 and ν_3 of the ${}^2A'$ states.

REFERENCES

1. D.E. Milligan and M.E. Jacox, *J. Chem. Phys.*, **38**, 2687 (1963).
2. R.K. Ritchie and A.D. Walsh, *Proc. Roy. Soc., (Lond.)*, **A267**, 395 (1962).
3. R.K. Ritchie, A.D. Walsh, and P.A. Warsop, *Proc. Roy. Soc., (Lond.)*, **A266**, 257 (1962).
4. A.E. Douglas and K.P. Huber, *Can. J. Phys.*, **43**, 74 (1965).
5. A.D. Walsh, *J. Chem. Soc.*, **8**, 2288 (1953).
6. K.H. Becker, E.H. Fink, et al., *J. Chem. Phys.*, **60**, 4623 (1974).
7. H.E. Hunziker and H.R. Wendt, *J. Chem. Phys.*, **60**, 4622 (1974).
8. K.H. Becker, E.N. Fink, et al., *J. Chem. Lett.*, **54**, 191 (1978).
9. P.A. Freedman and W.J. Jones, *J. Chem. Soc. Faraday Trans.*, **11**, No. 72, 207 (1976).
10. R.P. Tuckett, P.A. Freedman, et al., *Mol. Phys.*, **37**, No. 2, 379 (1979).
11. V.P. Bulatov, et al., *Kratkie soobscheniya po flzike*, No. 8, 46 (1986).
12. J.W. Swensson, et al., *The Solar spectrum from 7498 to 12016 A. Table Measures and Identifications Liege*, Belgique (1970).
13. G. Herzberg, *Electronic Spectra and Electronic Structure of Polyatomic Molecules*, Van Nostrand, N.Y. 1966 [in Russian, Mir, Moskow, (1969)].
14. S. Salito, *J. Mol. Spectr.*, **65**, 229 (1977).
15. C.E. Barnes, J.M. Brown, et al., *J. Mol. Spectr.*, **72**, 86 (1972).
16. K. Nagal, Y. Endo, et al., *J. Mol. Spectr.*, **89**, 520 (1982).
17. J.W.C. Johns, A.R.W. McKellar, et al., *J. Chem. Phys.*, **68**, 3957 (1978).
18. G. Herzberg, *Vibration and Rotayion Spectra of Poliyatomic Molecules* [in Russian, Izdatinlit, Moscow (1949)].
19. K.L. Holstein, E.H. Fink, et al., *J. Mol. Spectr.*, **99**, 231 (1983).